



Universiteit  
Leiden  
The Netherlands

## Bioorthogonal click chemistry to visualize an immunogenic HLA-A2-restricted hepatitis B virus epitope in human monocyte-derived dendritic cells

Mostert, T.P.; Kessler, A.L.; Luijten, R.J.; Doelman, W.; Isendoorn, M.M.E.; Filippov, D.V.; ... ; Buschow, S.I.

### Citation

Mostert, T. P., Kessler, A. L., Luijten, R. J., Doelman, W., Isendoorn, M. M. E., Filippov, D. V., ... Buschow, S. I. (2025). Bioorthogonal click chemistry to visualize an immunogenic HLA-A2-restricted hepatitis B virus epitope in human monocyte-derived dendritic cells. *Journal Of Immunology*. doi:10.1093/jimmun/vkaf312

Version: Publisher's Version

License: [Creative Commons CC BY 4.0 license](https://creativecommons.org/licenses/by/4.0/)

Downloaded from: <https://hdl.handle.net/1887/4285564>

**Note:** To cite this publication please use the final published version (if applicable).

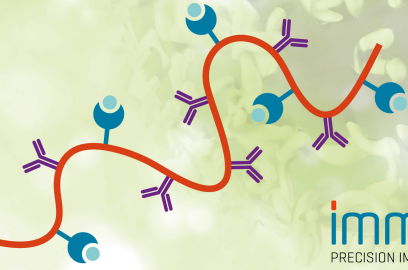
# Bioorthogonal click chemistry to visualize an immunogenic HLA-A2-restricted hepatitis B virus epitope in human monocyte-derived dendritic cells

Thijmen P Mostert, Amy L Kessler, Robbie J Luijten, Ward Doelman, Marjolein M E Isendoorn, Dmitri V Filippov, Sander I van Kasteren, Sonja I Buschow

**Antigen-Specific T Cell Activation and Expansion**

NEW Xynapse™ Reagents  
Mimic the TCR Immunological Synapse

LEARN MORE



The diagram illustrates the TCR Immunological Synapse. It shows two cells: a T cell on the left and a dendritic cell on the right. The T cell's T-cell receptor (TCR) is shown as a red curved line with blue circular ends, interacting with a peptide-MHC complex (purple Y-shaped structures) on the dendritic cell's surface. The dendritic cell also has blue circular structures on its surface. The background is a light green with a subtle leaf pattern.

**immuDEX®**  
PRECISION IMMUNE MONITORING

# **Bioorthogonal click chemistry to visualize an immunogenic HLA-A2-restricted hepatitis B virus epitope in human monocyte-derived dendritic cells**

Thijmen P. Mostert  <sup>1,\*,\*\*</sup>, Amy L. Kessler  <sup>2,3,\*\*\*</sup>, Robbie J. Luijten<sup>2</sup>, Ward Doelman  <sup>1,4</sup>, Marjolein M. E. Isendoorn<sup>5</sup>, Dmitri V. Filippov<sup>5</sup>, Sander I. van Kasteren  <sup>1,6,‡</sup>, and Sonja I. Buschow  <sup>2,\*,‡</sup>

<sup>1</sup>Department of Chemical Biology & Immunology, Leiden Institute of Chemistry, Leiden University, Leiden, 2333 CC, The Netherlands

<sup>2</sup>Department of Gastroenterology and Hepatology, Erasmus MC University Medical Center Rotterdam, Rotterdam, The Netherlands

<sup>3</sup>Present address: Biomolecular Mass Spectrometry and Proteomics, Bijvoet Center for Biomolecular Research and Utrecht Institute for Pharmaceutical sciences, University of Utrecht, Padualaan 8, The Netherlands

<sup>4</sup>Present address: Department of clinical pharmacology and toxicology, Leiden University Medical Center, Albinusdreef 2, 2333 ZA Leiden, The Netherlands

<sup>5</sup>Department of Bio-organic Synthesis, Leiden Institute of Chemistry, Leiden University, Leiden, 2333 CC, The Netherlands

<sup>6</sup>Institute of Chemical Immunology, Leiden Institute of Chemistry, Leiden University, Leiden, 2333 CC, The Netherlands

\*Corresponding Author: Department of Gastroenterology & Hepatology, Erasmus MC University Medical Center Rotterdam, P.O. Box 2040, 3000 CA, Rotterdam, The Netherlands. Email: S.Buschow@erasmusmc.nl

\*\*These authors contributed equally.

<sup>‡</sup>These authors contributed equally.

## Abstract

Peptide-based therapeutic vaccines exploit cross-presentation by dendritic cells for the induction of effective T cell responses. Their clinical success, however, has been limited due to incomplete understanding of antigen processing and presentation (APP). Bioorthogonal chemistry (BOC) uses chemical "click" reactions that can be performed selectively without interference of the cellular environment. A "click handle" can be incorporated into a biomolecule with only minor effects on its characteristics, allowing selective visualization and tracking of the biomolecule. We generated 10 analogues of the HLA-A2-restricted, immunogenic hepatitis B virus-derived epitope HBCAg<sub>18-27</sub> by replacing each amino acid with the click handle homopropargylglycine. Each analogue was tested for (1) peptide binding affinity to HLA-A2, (2) preservation of immunogenicity, and (3) accessibility for on-cell click reactions. Lastly, we performed a proof-of-concept experiment in which we demonstrate the feasibility of BOC for APP studies. All amino acids could be modified with the click handle without loss of HLA binding. Furthermore, 7 out of 10 analogues retained cognate T cell recognition. Two of the most promising analogues were tested and demonstrated to be accessible for on-cell click as well as suitable for long peptide processing and presentation studies. To our knowledge, we are the first to show the feasibility of BOC to study APP in the human setting. With BOC techniques, we may now be able to sensitively follow antigen routing by visualizing the intracellular location of (long) peptides. Furthermore, this tool enables direct and quantitative epitope studies in a T cell-independent manner.

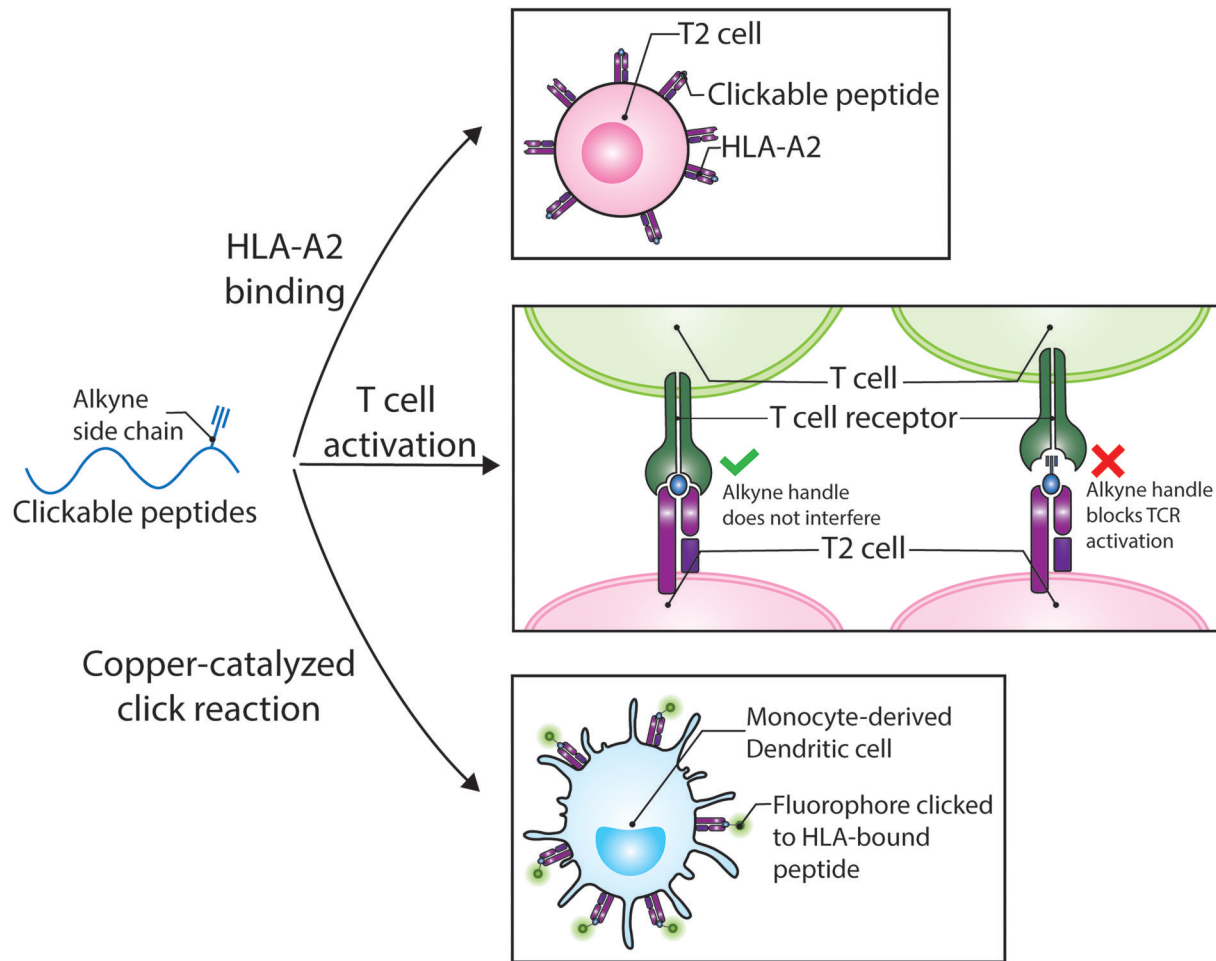
**Keywords:** major histocompatibility antigen (MHC), biorthogonal click chemistry, antigen processing and presentation, hepatitis B virus (HBV), core antigen (HBcAg)

Received: January 17, 2025. Accepted: October 24, 2025

© The Author(s) 2025. Published by Oxford University Press on behalf of The American Association of Immunologists.

© The Author(s) 2023. Published by Oxford University Press on behalf of The American Association of Immunologists. This is an Open Access article distributed under the terms of the Creative Commons Attribution License (<https://creativecommons.org/licenses/by/4.0/>), which permits unrestricted reuse, distribution, and reproduction in any medium, provided the original work is properly cited.

## Graphical abstract



## Introduction

Antigen processing and presentation (APP) is the process whereby cells produce peptides from protein antigens and present these on their major histocompatibility complexes (MHC; also known as human leukocyte antigen (HLA) in humans).<sup>1–3</sup> Recognition of such a peptide-HLA (pHLA) by a T cell through its unique T cell receptor (TCR) is the first and key event in T cell activation, driving the adaptive immune response against the antigen that the peptide originated from.<sup>4</sup> APP is a key target for biomedical interventions aiming to (re)initiate or stop immune responses against specific antigens via prophylactic and therapeutic vaccination strategies.<sup>5</sup> For the latter, promising results have been obtained for the treatment of viral infections, cancer and autoimmune disease.<sup>6–8</sup> Understanding the APP pathways, and particularly what parameters influence how much of a given pHLA is presented by an APC, is therefore of vital importance for improving vaccination strategies.

The mechanisms underlying APP are highly complex and depend on the source of the antigen and the cell type presenting the antigen.<sup>1–3</sup> Briefly, in the canonical route of APP occurring in most cells of the body, endogenously synthesized proteins are co-translationally degraded by the proteasome and the resulting peptides are loaded onto HLA class I (HLA-I) in the endoplasmic reticulum. The pHLA-I complexes are transported to the cell surface and presented to CD8<sup>+</sup> cytotoxic T cells. Contrarily, professional antigen presenting cells

(APCs), that are uniquely able to prime T cells, internalize and degrade exogenous antigens and load derived peptides onto HLA class II (HLA-II) for presentation to CD4<sup>+</sup> T helper cells, and on HLA-I for presentation to CD8<sup>+</sup> T cells. The latter, that is, the presentation of peptides from exogenous antigens on HLA-I, is called cross-presentation.<sup>9,10</sup> APCs excel at cross-presentation, and this allows them to prime CD8<sup>+</sup> T cells without being infected themselves. In APCs, HLA-I and -II peptides can be generated in the endosomal system, but for cross presentation, the proteasome may also be involved. Antigen size and form (eg, particulate, protein, or peptide) and the presence of pathogen-associated molecular patterns (PAMPs) can affect the route and efficiency of antigen (cross)-presentation and hence may determine vaccine efficacy.<sup>11–13</sup> The rules dictating (cross)-presentation, however, have not been fully resolved.<sup>9,10</sup>

One key problem in the study of APP is that there are few robust methods to quantify how many peptides appear on the surface of an APC and at what rate. Traditionally, T cells have been used as a readout: antigen-specific T cells are stimulated by an APC presenting a given amount of a particular antigen and their activation is measured via cell surface markers or cytokine secretion to infer the relative amounts of presented pHLA. This approach, however, is restricted by T cell clone availability and absolute quantification is impossible, as each T cell receptor will have a different functional avidity and hence pHLA requirement. Furthermore, T cell

activation is also biased by the expression of co-stimulatory molecules and cytokines by APCs, which can affect the strength of T cell activation by a given quantity of pHLa. In addition, T cells sense only the end point of the very complex APP pathway and cannot be used to study intracellular events.

To combat this T cell “addiction” when studying APP, multiple T cell-independent methods have been developed. These include antibodies that bind specific pHLa, often with modest affinity.<sup>14,15</sup> These still do not, however, yield any information on the intracellular mechanics of APP preceding HLA peptide loading. One popular approach to study this part of the APP has been the conjugation of “visible” proteins, such as HRP<sup>16</sup> and luciferase,<sup>17</sup> to the antigen of interest. These can then be followed inside the cell (while intact, at least). To also visualize the parts of the APP pathways where these visible proteins are degraded (and hence have become invisible), the conjugation of small molecules/fluorophores to antigens of interest has been explored extensively. However, the conjugation of these relatively bulky, charged, and/or hydrophobic fluorophores can impact the biophysical and -chemical properties, and with that the immunological properties, of the antigen and how it is subject to APP. Conjugation of small molecule fluorophores also results in changes to the antigen, particularly its conformation.<sup>18</sup> We have, for example, previously shown that APP of fluorophore-modified antigens differs significantly from unmodified antigen, likely the result of protein unfolding induced by the chemical modification reaction.<sup>19</sup> Moreover, due to their size, fluorophores affect loading of the processed peptides on HLA, and/or recognition by a TCR cognate for the unmodified antigen. Thus, there is an unmet need for a way to track antigens through APP pathways without interfering with HLA loading and TCR recognition. Such a tool would allow for more in-depth studies on the mechanisms that govern APP.

We and others have hypothesized that the Nobel Prize-winning bioorthogonal chemistry (BOC) could be ideally suited to visualize/follow peptide antigens within a cell or even in the pHLa complex without changing APP or T cell recognition.<sup>19–23</sup> Bioorthogonal click reactions are chemical reactions that can be performed selectively in complex cellular environments without interference from cellular components.<sup>24–27</sup> One of the most widely used click reactions is the copper (I)-catalyzed azide-alkyne cycloaddition (CuAAC).<sup>28,29</sup> To exploit this click reaction in biological systems, it is necessary to incorporate either an azide or alkyne “click handle” in the biomolecule of interest. This click handle can react with its counterpart to form a 5-membered triazole ring,<sup>28,29</sup> allowing ligation of, for example, an azide-functionalized fluorophore to an alkyne-modified biomolecule, at any stage during the biological process of interest, post cell fixation (as the copper needed for the reaction is highly toxic). Such click handles are small and therefore minimally alter the biophysical and -chemical properties of the biomolecule they are incorporated in. Hence, they will be a much better mimic of the native biomolecule than the fluorophore-modified variant. Moreover, they are biologically inert, and are stable in the harsh environments found in the antigen presentation pathways for at least 24 h.<sup>27,30</sup> For proteins or peptides, click handles are easily incorporated via non-canonical amino acids (eg, the alkyne-functionalized amino acid homopropargylglycine (Hpg)).<sup>31</sup> Bioorthogonal click chemistry has, for example, already been used to study the uptake and intracellular fate of proteins,<sup>19</sup>

lipids,<sup>32</sup> exogenous RNA,<sup>33</sup> and sugars,<sup>34</sup> as well as the metabolic labeling of DNA and RNA.<sup>35,36</sup> However, both peptide-HLA binding and TCR recognition are highly specific processes, where the modification of one residue in the peptide can abolish binding to HLA and/or recognition by the TCR. Yet our group has previously developed a click reactive MHC class I epitope based on the well-known murine OVA SIINFEKL peptide.<sup>23</sup> Unfortunately, this reactive epitope was no longer recognized by the cognate TCR, which limits its use. Recently, a HLA-DR1 (HLA class II)-restricted click reactive epitope has been used to directly assess HLA-II presentation, albeit without assessment of its ability to drive T cell activation.<sup>20</sup> So far, click chemistry has never successfully been applied to study human HLA-I APP.

In the present study, we have designed and characterized click-reactive analogues of the clinically relevant, well studied, high affinity, and HLA-A2-restricted Hepatitis B virus core antigen-derived HBcAg<sub>18–27</sub> peptide. We modified each position in this immunodominant epitope with a bioorthogonally reactive amino acid (Hpg). These click reactive peptides were assessed for both HLA-A2 binding capabilities and T cell activating potential. To our excitement, it was found that Hpg-substitution at positions 6 and 9 yielded peptides that could be both detected by on-surface click chemistry and at the same time could still activate T cells specific for the wild-type (WT) epitope. Finally, in order to show the applicability of our novel approach, we incorporated the click epitopes in synthetic long peptides (SLPs) that are used for therapeutic vaccination and assessed the uptake, degradation, and the surface presentation of SLP-originated epitopes by monocyte-derived dendritic cells (moDCs). Our work puts forward click variants of the HBcAg<sub>18–27</sub> epitope as a new model system to study APP directly in a T cell-independent manner.

## Materials and methods

### Peptides

Click reactive and WT HBcAg<sub>18–27</sub> peptides (sequence: FLPSDFFPSV; for click analogues each position was once modified with Hpg) were purchased from Pepscan (>90% purity) or synthesized in house (see [supplemental methods](#)). Cytomegalovirus-pp65<sub>495–503</sub> peptide (CMV-pp65<sub>495–503</sub>, sequence: NLVPMVATV) was purchased from Peptide 2.0 (>95% purity). Survivin<sub>96–104</sub> peptide (sequence: LTLGEFLKL) was purchased from Peptide 2.0 (crude). SLPs (sequence: MDIDPYKEFGATVELLSFLPSDFFPSVRDLLDTASAL), either containing Hpg at positions 6 or 9 in the core epitope (bold in the sequence) or left unmodified, were synthesized in house (see [supplemental methods](#)). All HBcAg<sub>18–27</sub> variants, CMV-pp65<sub>495–503</sub>, and SLPs were dissolved in 100% DMSO (Sigma-Aldrich), whereas Survivin<sub>96–104</sub> was dissolved in 10% DMSO in H<sub>2</sub>O. All peptides were dissolved to a stock concentration of 10 mM and stored at -20 °C.

### HLA-A2 stabilization assays of bioorthogonal HBcAg<sub>18–27</sub> peptides using T2 cells

The T2 cell line (174 × CEM.T2, ATCC CRL-1992, kindly provided by prof. dr. Debets)<sup>37</sup> was cultured in T2 cell medium (RPMI-1640 supplemented with 2 mM ultraglutamine (Lonza), 10% heat inactivated fetal calf serum (FCS, PAN Biotech), and 100 U/ml penicillin/streptomycin (P/S, Gibco)). The cells were maintained in a humidified incubator at

37°C, 5% CO<sub>2</sub>, and grown to a maximal density of 1.5 × 10<sup>6</sup> cells/ml.

Cells were harvested and resuspended to 1.5×10<sup>6</sup> cells/ml in serum-free T2 cell medium supplemented with 6 µg/ml human β2-Microglobulin (B2M, Bio-Rad). A serum-free method was used, as bovine B2M in culture medium can interact with human HLA-I complexes.<sup>38</sup> Peptides were diluted in serum-free T2 cell medium to twice the required end concentration. As negative control, DMSO was diluted in serum-free culture medium to the same concentrations found in the peptide dilutions (0.5%–0.002%). The cells were plated in a 96-well round-bottom plate (0.15×10<sup>6</sup> cells/well) and incubated 1:1 with the diluted peptides or DMSO for 3 h at 37°C, 5% CO<sub>2</sub> (final concentrations: 0.75×10<sup>6</sup> cells/ml, 3 µg/ml B2M, indicated peptide concentrations). The cells were subsequently washed with ice-cold FACS buffer (1× phosphate buffered saline (PBS, HyClone) + 1% bovine serum albumin (BSA, Sigma-Aldrich) + 1% human serum (PAN Biotech) + 0.02% sodium azide (Sigma-Aldrich)) and stained with anti-human HLA-A2 antibody conjugated to Alexa Fluor 488 (BB7.2, Bio-Rad, 1 µg/ml in FACS buffer) for 30 min at 4°C. Cells were washed with ice-cold FACS buffer prior to analysis on a BD FACSCanto<sup>TM</sup> II Cell Analyzer. All flow cytometry data was analyzed with FlowJo v10.7 (Becton, Dickinson & Company). Mean fluorescence intensity (MFI) of Alexa Fluor 488 was determined as a measurement for surface HLA-A2 levels. The percentage MFI increase upon peptide binding was calculated to correct for background levels of surface HLA-A2 in the following manner: %MFI increase=((MFI (Peptide)-MFI (DMSO))/MFI(DMSO)) ×100%. Each assay was set up in triplicate. Mean, standard error of the mean (SEM), and EC<sub>50</sub> values were calculated with GraphPad Prism 8.0.2 for Windows (GraphPad Software). EC<sub>50</sub> values and simulated binding curves were determined with nonlinear regression curve fits using the Log(agonist) vs response—Find EC anything function with the method of least squares. The F value was constrained to 50 to calculate the EC<sub>50</sub> and the bottom value was constrained to 0, as the used data were already corrected for background. All error bars correspond to the SEM.

#### HBcAg<sub>18-27</sub>-specific T cell activation assays with bioorthogonal peptides

T2 cells (0.4×10<sup>6</sup> cells/ml) were pulsed with 1 µM HBcAg<sub>18-27</sub> (WT and click variants) in serum-free T2 cell medium supplemented with 3 µg/mL B2M for 1 h at 37°C, 5% CO<sub>2</sub>. As a positive control T2 cells were incubated with 10 µM CMV-pp65<sub>495-503</sub>. Negative controls of 10 µM Survivin<sub>96-104</sub> as irrelevant epitope and the corresponding DMSO concentration (0.01%) found in the HBcAg<sub>18-27</sub> samples were included. After incubation the cells were washed once with cold serum-free T2 cell medium and once with cold T cell medium (IMDM (Lonza) supplemented with 2 mM ultraglutamine (Lonza), 2% human serum (PAN Biotech), and 100 U/ml P/S). Subsequently, the cells were taken up in cold T cell medium and incubated in a 1:1 ratio (cell: cell, 0.4×10<sup>6</sup> total cells/ml) with CMV-pp65<sub>495-503</sub>-specific T cells or with the same T cell clone retrovirally transduced with a HBcAg<sub>18-27</sub>-specific T cell receptor (clonotype Vα17-P2A-Vβ12-4 kindly provided by prof. dr. A. Bertoletti;<sup>39</sup> transduction performed as published<sup>40,41</sup>) for 20 h at 37°C, 5% CO<sub>2</sub>. After incubation the supernatant was harvested and stored at -20°C for later interferon gamma (IFN-γ) ELISA. Assays were set up in duplicate.

#### Interferon gamma (IFN-γ) ELISA

A human IFN-γ uncoated ELISA kit was purchased from Invitrogen. The INF-γ ELISAs were performed according to the manufacturer's protocol. Samples were diluted 1:2 or 1:10. The absorbance of the wells at 450 nm was measured using a TECAN Infinite<sup>®</sup> M Nano plate reader. Absorbance values were corrected for the blank and IFN-γ concentrations were calculated using the serial dilution of the IFN-γ standard. The mean and SEM were calculated with GraphPad Prism. Error bars correspond to the SEM.

#### Preparation of click mix

Click mix was always prepared fresh before use by the addition of the following reagents in the given order: CuSO<sub>4</sub> (Sigma Aldrich), sodium ascorbate (Sigma Aldrich), tris (3-hydroxypropyltriazolyl-methyl)amine (THPTA, Sigma Aldrich or synthesized in house), aminoguanidine (ACROS Organics), HEPES (Lonza), and azide-fluorophore. The click mix for click reactions directly on cells has the following concentrations: 1 mM CuSO<sub>4</sub>, 10 mM sodium ascorbate, 1 mM THPTA, 10 mM aminoguanidine, 96 mM HEPES, and 10 µM azide-fluorophore.

#### PBMC isolation and moDC differentiation

For the generation of moDCs, peripheral blood mononuclear cells (PBMCs) were isolated from buffy coats from healthy donors, obtained from the local blood bank. All donors gave written informed consent. PBMCs were isolated from the buffy coat using Ficoll-Paque (GE Healthcare) density gradient centrifugation. Monocytes were isolated from the PBMCs by adherence to cell culture flasks. For this, PBMCs were resuspended in attachment medium (IMDM supplemented with 2% human serum, 2 mM ultraglutamine, and 100 U/ml P/S), and cells were allowed to adhere to the flask for 1 h at 37°C, 5% CO<sub>2</sub>. The non-adherent cells (the peripheral blood lymphocytes) were subsequently removed. The attached monocytes were cultured over the course of 6 to 7 d in differentiation medium (IMDM supplemented with 2 mM ultraglutamine, 8% FCS, 100 U/ml P/S, 500 IU/ml IL4 (Peprotech) and 800 IU/ml GM-CSF (Peprotech)). On day 3, the differentiating moDCs were harvested, counted, and seeded for the experiments in fresh differentiation medium.

#### On-surface click of peptide-loaded HLA-A2<sup>+</sup> moDCs

On day 3 of the differentiation protocol, moDCs were seeded out in fresh differentiation medium at a concentration of 2.5 × 10<sup>5</sup> cell/well in 12-well plates. LPS-supplemented (100 ng/ml; Invivogen) differentiation medium was added on day 6 for 24 h to induce moDC maturation. Matured moDCs, according to each sample condition, were pre-treated with 10 µM Rottlerin (Sigma-Aldrich) for 30 min prior to incubation with peptides (25 µM) and fluorescently labeled BSA (10 µg/ml, Alexa Fluor 647-conjugate, Invitrogen) for 3 h at 37°C, 5% CO<sub>2</sub>. To control conditions, medium/DMSO was added in corresponding concentrations (0.25%).

After incubation, cells were harvested with ice-cold PBS, transferred to a 96-well round bottom plate, and fixed for 15 min at room temperature (RT) in 2% PFA. From here onward, all centrifugation in between steps were done at 290 ×g for 5 min at 4°C. To quench the PFA, cells were incubated with 100 mM glycine (Fisher Scientific) in PBS for 15 min at RT. Cells were subsequently blocked with 1% BSA and 1% fish skin gelatin (w/v; Sigma-Aldrich) for 15 min at RT,

washed with PBS (RT) and clicked for 45 min at RT with CalFluor 488 (Click Chemistry Tools) as fluorophore. After the click reaction, cells were blocked once more as described above and washed with FACS buffer.

MoDCs not pulsed with peptides were assessed for viability and maturation marker expression by flow cytometry. These samples were labeled with anti-HLA-DR conjugated to PE (LN3, 17.5 ng/ml, eBioscience), anti-CD40 conjugated to APC (5C3, 240 ng/ml, eBioscience), and anti-HLA-I conjugated to Pacific Blue (W6/32, 10 µg/ml, Biolegend) in FACS buffer for 30 min at 4 °C in the dark. Cells were washed with FACS buffer and resuspended in FACS buffer. All samples were analyzed on a BD FACSCanto™ II Cell Analyzer.

### Uptake and degradation of SLPs by moDCs analyzed by flow cytometry

MoDCs (not selected for HLA-A2 expression) were seeded in 24-well plates ( $4 \times 10^5$  cells/well in 400 µl of differentiation medium supplemented with fresh IL4 and GM-CSF) on day 3 of the differentiation protocol. On day 6, SLPs or minimal epitopes were added to a final concentration of 10 µM in fresh differentiation medium. To mimic SLP-based vaccines, 10 µM of the Toll like receptor (TLR) 1/2 ligand UPam (Pam3CysSK4 in which in the N-palmitoylate the α-amino group of the terminal cysteine residue is replaced by an alkylurea, also known as Amplivant®, synthesized as described previously<sup>42,43</sup>) was added. To assess differences in the endocytic capacity of the cells, the medium with peptides and UPam was also supplemented with 10 µg/ml fluorescently labeled BSA (Alexa Fluor 647-conjugate, Invitrogen). As a negative control, moDCs were incubated with vehicle (DMSO) instead of the peptide and UPam (BSA-Alexa Fluor 647 was present in these conditions). The cells were pulsed with the peptides and UPam for 1 or 3 h at 37 °C, 5% CO<sub>2</sub>. Following the incubation, the medium was removed by centrifugation (5 min, 362 ×g), and the cells were washed once with PBS. The cells were then harvested and split into two parts. Half of the cells were fixed with 2% PFA in PBS for 15 min at RT and stored overnight in 0.5% PFA in PBS at 4 °C. The other half of the cells were re-plated in new 24-well plates in fresh differentiation medium and chased for 20 h at 37 °C, 5% CO<sub>2</sub>. Following the chase period, the medium was removed by centrifugation and the cells were washed with PBS. The cells were then harvested and fixed with 2% PFA in PBS for 15 min at RT.

To analyze the uptake of the SLPs and minimal epitopes, the PFA was quenched with 100 mM glycine (Fisher Scientific) in PBS for 15 min at RT in the dark (all subsequent steps were performed in the dark as much as possible). The cells were washed twice with PBS and permeabilized with 0.05% saponin (VWR chemicals) in PBS for 20 min at RT. The cells were then washed twice with PBS and clicked for 45 min at RT with CalFluor 488 as fluorophore. Subsequently, the click mix was washed away twice with PBS, allowing at least 2 min incubation for each wash. The cells were then blocked for 1 h at RT with 1% BSA in PBS, followed by a wash with FACS buffer. The cells were resuspended in FACS buffer and analyzed on a BD FACSCanto™ II Cell Analyzer.

To assess the maturation status of the moDCs induced by the UPam, moDCs were incubated with either 10 µM UPam, 100 ng/ml LPS as positive control, or DMSO vehicle control as negative control in fresh differentiation medium, for 3 h

and chased for 20 h at 37 °C, 5% CO<sub>2</sub>. The medium was subsequently removed by centrifugation, the cells were washed once with PBS, harvested, and labeled with a Live/Dead viability dye in AmCyan (1:200, Invitrogen), anti-HLA-DR conjugated to PE (LN3, 17.5 ng/ml, eBioscience), anti-CD40 conjugated to PerCP-eFluor710 (5C3, 75 ng/ml, eBioscience), and anti-HLA-I conjugated to Pacific Blue (W6/32, 10 µg/ml, Biolegend) in FACS buffer for 30 min at 4 °C in the dark. Subsequently, the cells were washed with FACS buffer, resuspended in FACS buffer, and analyzed on a BD FACSCanto™ II Cell Analyzer.

### Uptake and degradation of SLPs by moDCs analyzed by confocal microscopy

MoDCs (not selected for HLA-A2 expression) were seeded in Ibidi 8-chamber microscopy slides (IbiTreat for optimal cell adhesion,  $1.5 \times 10^5$  cells/well in differentiation medium supplemented with fresh IL4 and GM-CSF) on day 3 of the differentiation protocol. On day 6, SLPs or minimal epitopes were added to a final concentration of 10 µM together with UPam at a final concentration of 10 µM in fresh differentiation medium and the cells were incubated with peptide and UPam for 3 h at 37 °C, 5% CO<sub>2</sub>. The medium with the peptides was then aspirated, the cells were washed once with PBS, fresh differentiation medium was added and the cells were incubated for 20 h at 37 °C, 5% CO<sub>2</sub> to allow time for processing of the peptides. After the chase period the medium was removed, the cells were washed once with PBS and the cells were fixed with 2% PFA in PBS for 15 min at RT. The fixation solution was then replaced with 0.5% PFA in PBS and the samples were stored overnight at 4 °C. Subsequently, the storage buffer was aspirated and the PFA was quenched with 100 mM glycine (VWR Chemicals) in PBS for 15 min at RT. After quenching, the cells were washed twice with PBS and permeabilized with 0.05% saponin (EMD Millipore) in PBS for 20 min at RT and washed twice again with PBS, with each wash incubated for 5 minutes at RT. The cells were stained with 1× clickmix with AZDye 488 azide (Click Chemistry Tools) as fluorophore for 45 min at RT in the dark. All subsequent steps were performed in the dark to minimize bleaching of the fluorophores. The cells were washed twice with PBS, allowing at least 2 min of incubation each time, after which blocking buffer (10% goat serum (EMD Millipore) and 0.05% saponin in PBS) was added for 30 min at RT. After aspiration of the blocking buffer, the cells were incubated for 1 h at RT with Rabbit anti-LAMP1 antibody (Sigma Aldrich, polyclonal, diluted 1:100 in 5% goat serum and 0.05% saponin in PBS), followed by 3 washes with 1% goat serum and 0.05% saponin in PBS. Secondary goat anti-Rabbit IgG antibody conjugated to Alexa Fluor 647 (Invitrogen, diluted 1:500 in 5% goat serum and 0.05% saponin in PBS) was added and incubated for 1 h at RT. Subsequently, the cells were washed 3 times with 1% goat serum and 0.05% saponin in PBS, allowing 5 min incubation for each wash. The cells were then stained with Ultra-LEAF anti-human HLA-ABC (BioLegend, W6/32, 1 µg/ml in 5% goat serum and 0.05% saponin in PBS) for 1 h at RT, followed by washing twice with 1% goat serum and 0.05% saponin in PBS. Next, secondary goat anti-mouse IgG antibody conjugated to Alexa Fluor 555 (Invitrogen, diluted 1:500 in 5% goat serum and 0.05% saponin in PBS) was added and incubated for 1 h at RT. The cells were then washed once with 1% goat serum and 0.05% saponin in PBS and once with PBS.

Nuclei were counterstained with DAPI (1 µg/ml in PBS) for 10 min at RT, after which the cells were washed once with PBS, glycerol/DABCO was added, and samples were stored at 4 °C until imaging.

### Confocal microscopy and image analysis

Confocal microscopy was performed on an AR1 HD25 confocal microscope (Nikon), equipped with a Ti2-E inverted microscope, LU-NV Series laser unit, and CFI Plan Apo Lambda 100×/1.45 oil objective. Fluorophores were excited using the corresponding laser lines (DAPI: 405 nm; AZDye 488 azide: 488 nm; Alexa Fluor 555: 561 nm; Alexa Fluor 647: 647 nm). The Resonant scanner was used to acquire the images, whilst poisson noise was immediately removed by the built-in Nikon Denoise.ai software. Z-stacks were made from the bottom to the top of the cells in the field of view with steps of 0.175 µm (on average 76 slices, ranging from 40 to 137 slices). For the moDCs from the first donor 2 fields of view (FOVs) were imaged for the SLP conditions each and 1 FOV for the min. epitope conditions. For the moDCs from the second and third donors 5 FOVs were imaged for the SLP-P6 and -P9 conditions each, and 3 FOVs for the SLP-WT and all min. epitope conditions. There were, on average, 8 cells per FOV, ranging from 4 to 16 cells/FOV. The Volume View command in the NIS Elements software (Nikon) was used to create 3D rendered images of the Z-stacks. Brightness and contrast were adjusted identically for all images from the same donor to ensure the relative intensity remained the same. Images are presented as both a 2D cross section taken from the Z-stacks and a 3D representation.

Colocalization analysis of the click handle with HLA-I, LAMP1, and DAPI was performed using the JaCoP plugin in ImageJ.<sup>44</sup> The colocalization analysis was performed on both the 2D cross sections as well as on the 3D Z-stacks (to analyze colocalization in the 3D (volume) structure of the cell). The Manders' coefficients were calculated for the colocalization of click signal with DAPI, HLA-I, and LAMP1. The thresholds for the calculation of the Manders' coefficients were kept the same for all images from the same donor. The M<sub>1</sub> coefficient represents the fraction of the click signal overlapping with the markers, whereas the M<sub>2</sub> coefficient represents the fraction of the marker overlapping with the click signal.

## Results

### All click HBcAg<sub>18-27</sub> analogues retain HLA-A2-binding

For this proof-of-concept study, we investigated 10 analogues of the HLA-A2-restricted immunogenic epitope HBcAg<sub>18-27</sub>, derived from the hepatitis B virus core protein sequence (Table 1). In each of these peptides, one position was substituted for the alkyne-containing amino acid Hpg. To understand how this change affected subsequent experiments, we inspected solvent accessibility of the amino acid side-chains. This feature has been shown necessary for the successful bioorthogonal ligation of a peptide within the HLA binding groove.<sup>23</sup> To identify potential solvent-accessible residues, the crystal structure of the wild-type (WT) peptide HBcAg<sub>18-27</sub> bound to HLA-A2 (protein data bank (PDB) identifier 1HHH<sup>45</sup>) was analyzed in the UCSF Chimera software (Fig. 1A).<sup>46</sup> Based on this 3D structure, positions 1 (F), 4 (S), 5 (D), 8 (P), and 9 (S) were the most likely candidates for click ligation in the HLA complex because the sidechains

**Table 1.** Overview of the BOC-modified HBcAg<sub>18-27</sub> analogues used in this study.

Modification	Sequence	EC <sub>50</sub> (µM)
Wild-type	FLPSDFFPSV	0.17
Position 1 (F)	(Hpg)LPSDFFPSV	0.16
Position 2 (L)	F(Hpg)PSDFFPSV	0.20
Position 3 (P)	FL(Hpg)SDFFPSV	0.19
Position 4 (S)	FLP(Hpg)DFFPSV	0.15
Position 5 (D)	FLPS(Hpg)FFPSV	0.15
Position 6 (F)	FLPSD(Hpg)FPSV	0.12
Position 7 (F)	FLPSDF(Hpg)PSV	0.20
Position 8 (P)	FLPSDFF(Hpg)SV	0.30
Position 9 (S)	FLPSDFFP(Hpg)V	0.21
Position 10 (V)	FLPSDFFPS(Hpg)	0.37

Each position of the WT sequence was replaced with Hpg. EC<sub>50</sub> values of each peptide were determined by HLA binding titrations (Fig. 1C).

of these amino acids point outwards in the crystal structure; although this may differ for the Hpg analogues.

Hpg may affect the HLA binding capacity of the modified analogues. This was assessed by synthesizing the 10 Hpg-analogues and assessing their HLA-A2 binding affinity using a flow cytometry-based T2 HLA stabilization assay.<sup>37,47,48</sup> In this assay the increase of HLA-A2 surface levels is a measure for the stabilization of the HLA-A2 complex induced by the binding of exogenously added peptides. While internalization is required for antigen processing, the loading of minimal HLA epitopes, can already occur through peptide exchange on the cell surface.<sup>49-51</sup>

Incubation with the HBcAg<sub>18-27</sub> click analogues at 25 µM revealed that all positions, including anchor residues at position 2 and 10, can be modified without loss of HLA-A2 binding (Fig. 1B). Compared to the WT peptide, Hpg modification of positions 1, 2, 4, 5, and 8 slightly reduced HLA binding, whereas at position 6, binding affinity was slightly increased.

Next, the concentration at which each click analogue maximally stabilizes the HLA-A2 complex was determined (Fig. 1C). Peptide titrations were performed in batches that each included the WT peptide as internal reference. The data revealed that almost all analogues plateaued at a concentration of 1 µM, indicating maximal HLA stabilization. The half maximal stabilization (EC<sub>50</sub>) was subsequently calculated from the generated binding curves. Except for positions 8 and 10, all residues could be modified without large impact on their EC<sub>50</sub> values (Table 1).

### Most click HBcAg<sub>18-27</sub> analogues are recognized by the cognate TCR

The ideal pHLA-quantifying agent is both directly detectable, and can be “read out” in a T cell activation assay, to allow direct comparison of absolute peptide surface concentration and T cell activation. However, in studies of click-epitopes in mouse MHC-I, no variations could be made that allowed both clicking and T cell activation in a single assay.<sup>23</sup> We next assessed whether HBcAg<sub>18-27</sub>-alkyne analogues could still drive T cell activation. For this, we utilized clonally expanded cytomegalovirus-pp65<sub>495-503</sub> (CMV-pp65<sub>495-503</sub>)-specific CD8<sup>+</sup> T cells that were engineered to co-express a well-described HBcAg<sub>18-27</sub>-specific TCR,<sup>39,40</sup> and co-cultured those for 20 h with T2 cells pulsed with the click analogues (Fig. 2A). Interferon-γ (IFN-γ) levels in the supernatant were determined as a measure of CD8<sup>+</sup> T cell activation.

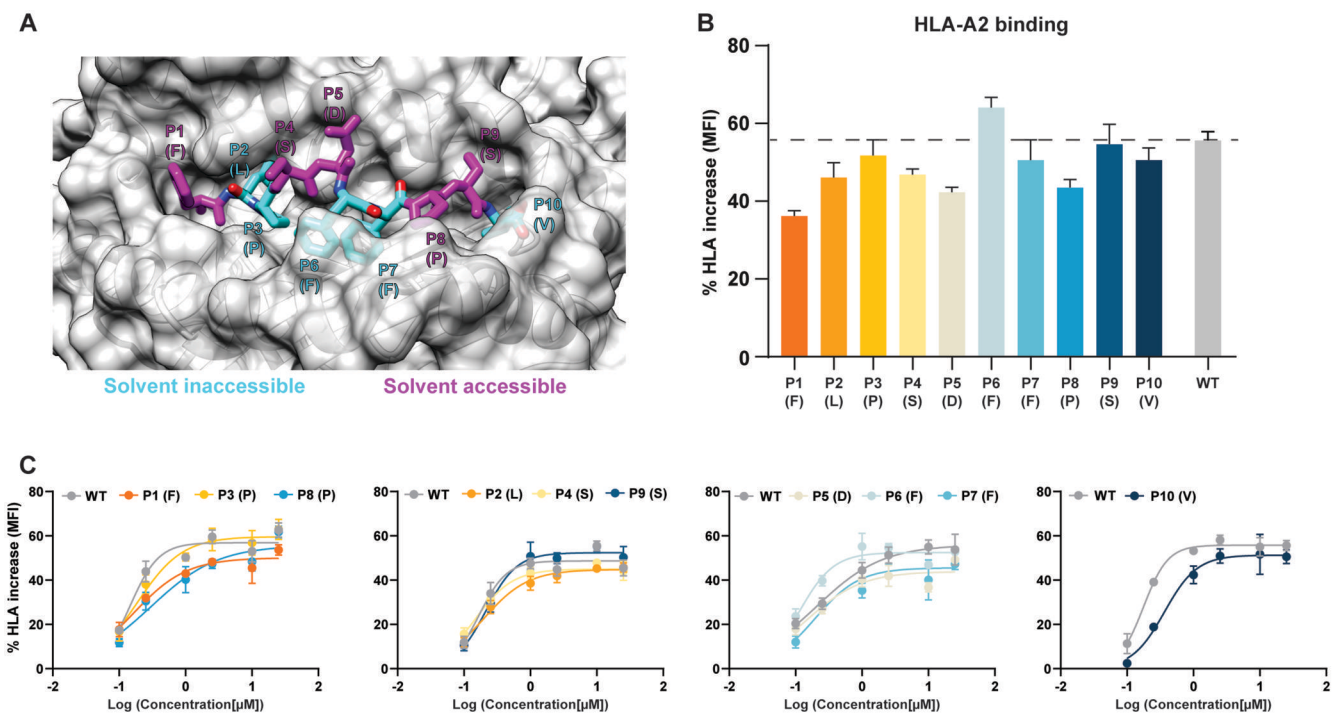


**Figure 1.** All click HBcAg<sub>18-27</sub> analogues bind to HLA-A2 as determined by the T2 assay. (A) The crystal structure of the WT HBcAg<sub>18-27</sub> peptide bound to HLA-A2 was rendered with UCSF Chimera software. Solvent inaccessible residues are visualized in blue, those solvent accessible are visualized in pink. (B) HLA-A2 stabilization on T2 cells by HBcAg<sub>18-27</sub> analogues at 25  $\mu$ M. Modified positions are indicated. Error bars correspond to the SEM of the technical triplicates. (C) EC<sub>50</sub> values as determined by peptide titrations on T2 cells, performed in batches. Each graph represents a separate batch measurement. The WT peptide was taken along in each batch. Lines correspond to fitted binding curves and error bars correspond to the SEM of the technical triplicates. Binding curves were fitted with the non-linear find ECanywhere function in Graphpad.

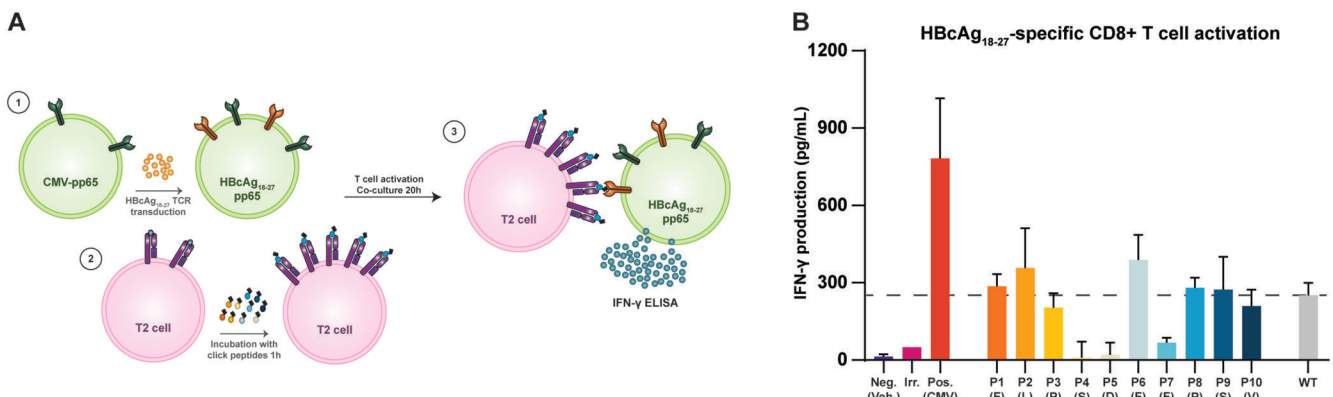


**Figure 2.** The majority of HBcAg<sub>18-27</sub> analogues are recognized by the cognate WT TCR. (A) A schematic overview of the experimental set-up. CMV-specific T cells were transduced with a HBcAg<sub>18-27</sub>-specific TCR and co-cultured with pulsed T2 cells for 20 h. T cell activation was read-out by measuring IFN- $\gamma$  levels in the supernatant. (B) HBcAg<sub>18-27</sub> TCR activation against all HBcAg<sub>18-27</sub> click analogues (1  $\mu$ M), negative control ("Neg."; DMSO), irrelevant peptide Survivin<sub>96-104</sub> ("Irr"; 10  $\mu$ M), or CMV-pp65<sub>495-503</sub> peptide ("Pos."; 10  $\mu$ M).  $N=3$  biological replicates with  $n=2$  technical replicates each, except the irrelevant Survivin peptide ( $N=1$  biological replicate,  $n=2$  technical replicates).

As expected, the CMV-pp65<sub>495-503</sub> peptide recognized by the native TCR outperformed other peptides, but significant T cell activation was also reached with the WT HBcAg<sub>18-27</sub> peptide. Interestingly, most residues within the HBcAg<sub>18-27</sub> peptide could be replaced with Hpg without loss of T cell activation (Fig. 2B). Modification of positions 4, 5, and 7, located in the middle region of the epitope, however, fully abolished IFN- $\gamma$  production, indicating their importance for TCR recognition. Of note, CMV-pp65<sub>495-503</sub>-specific T cells without the HBcAg<sub>18-27</sub>-specific TCR did not react with either the click or WT HBcAg<sub>18-27</sub> analogues (Fig. S1). These data indicate that click modification of the HBcAg<sub>18-27</sub>

peptide at positions 1, 2, 3, 6, 8, 9, and 10 are tolerated by this HBcAg<sub>18-27</sub>-specific TCR.

#### HBcAg<sub>18-27</sub> homopropargylglycine analogues P6 and P9 are available for click in the HLA binding groove

Tracking of antigen presentation ends with the loading of the epitope onto the HLA complex. Being able to perform the bioorthogonal ligation within the HLA binding groove is therefore essential to track the antigen throughout the entire processing pathway. To assess the reactivity of the different

epitopes, all HBcAg<sub>18-27</sub> Hpg analogues were first tested for their reactivity in solution with CalFluor 488, a quenched azide-based fluorophore which increases in fluorescence signal by two orders of magnitude upon CuAAC reaction with an alkyne (Fig. S2).<sup>52</sup> As shown by the fluorescent signal, all 10 analogues reacted with equal yield, whereas the “no peptide” and “WT” controls, as expected, did not give any undesired signal.

It was next assessed whether the click reaction could yield detectable signal on HLA-A2 expressing monocyte-derived dendritic cells (moDCs). In earlier work with click peptides for mouse MHC-I, poor signal-to-noise ratios were experienced when studying peptides bound to MHC.<sup>23</sup> It was therefore first assessed whether this issue also held true for our model peptide in the context of the HLA-A2 binding groove on moDCs. To ensure optimal experimental conditions (ie, large amounts of available HLA-A2), moDCs were matured with LPS. Maturation was confirmed using maturation markers CD40, HLA-I, and HLA-DR (Fig. 3A).

The easiest way to assess whether click peptides can be ligated in the context of HLA is by exploiting the surface exchange of minimal epitopes into HLA on the surface of mature moDCs. MoDCs, however, continuously sample their

environment by fluid-phase endocytosis (FPE), which could give a false positive signal. To prevent this, moDCs were pre-incubated for 30 min with the FPE-inhibitor Rottlerin,<sup>53,54</sup> which was also kept present during the peptide loading. The significant reduction of fluorescent bovine serum albumin (BSA) uptake confirmed Rottlerin potently inhibited FPE (Fig. 3B). Hence, the system was suitable to measure solely true signal from surface-exchanged, HLA-bound click peptides.

Based on the HLA binding assay and cognate TCR recognition, click epitopes P6 and P9 seemed the most promising all-round candidates for follow-up studies. To assess their clickability in HLA, LPS-matured and Rottlerin-treated moDCs were pulsed for 3 h with either WT HBcAg<sub>18-27</sub>, click analogues P6 and P9, or a click reactive variant of the murine ovalbumin (OVA) peptide SIINFEKL (OVA<sub>257-264</sub>), which does not bind HLA-A2:01, or DMSO (Fig. 3C). After cell fixation and CuAAC with the fluorophore CalFluor 488,<sup>52</sup> signal was observed for click HBcAg<sub>18-27</sub> epitopes P6 and P9 but not the OVA<sub>257-264</sub> peptide, indicating that these peptides can be ligated within the HLA binding groove rather than it being false positive signal due to peptide “stickiness.” Of note, for click analogue P6, Rottlerin significantly decreased background signal, and thus enhanced the signal-to-noise

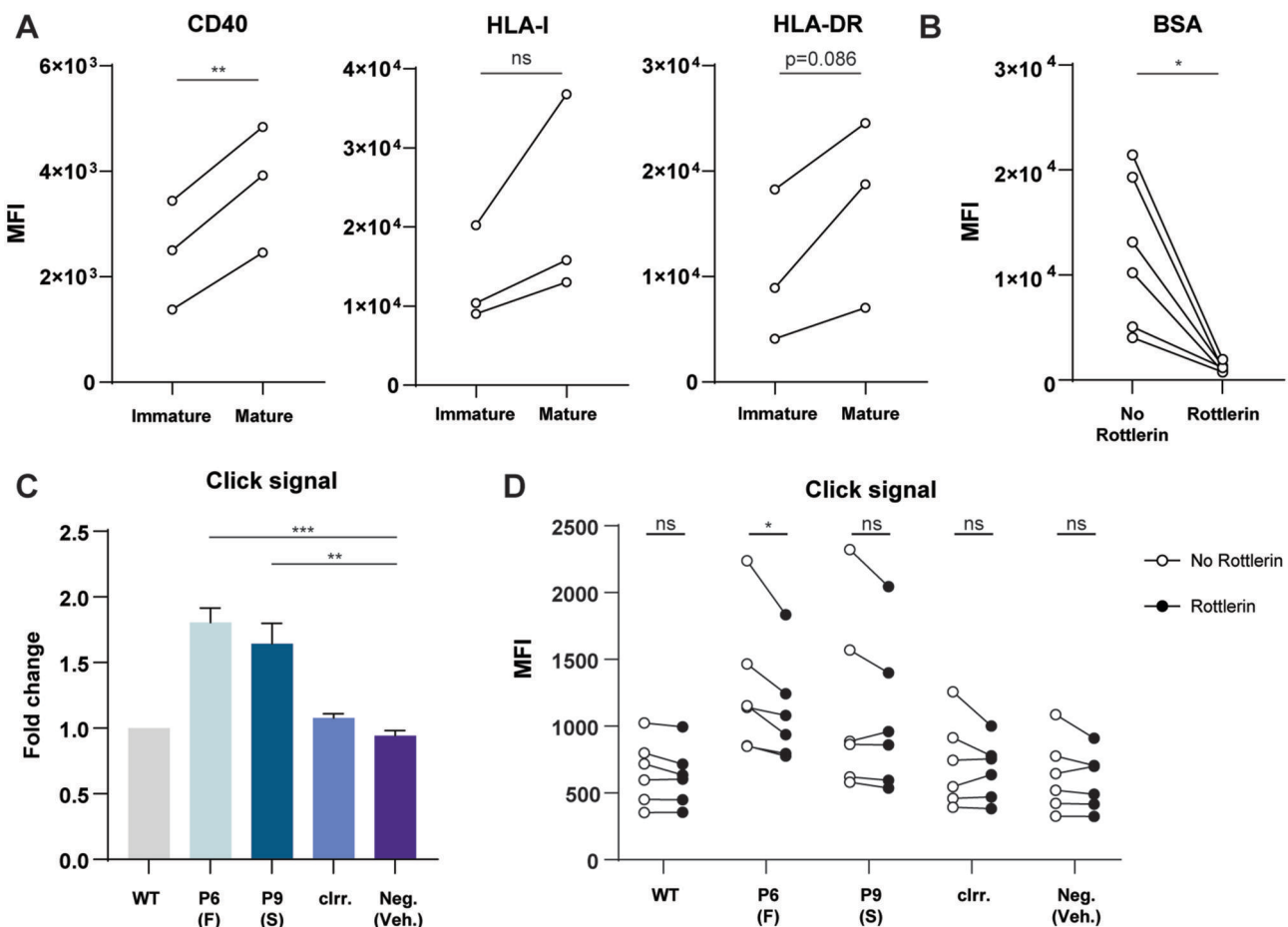


**Figure 3.** Click HBcAg<sub>18-27</sub> P6 and P9 are ligatable in the HLA-A2 binding groove. (A) Maturation status of LPS-stimulated (24 h) moDCs was assessed by the measurement of CD40, HLA-I and HLA-DR expression by flow cytometry.  $N=3$  biological replicates (with technical duplicates). (B) The efficacy of fluid phase endocytosis inhibition by Rottlerin was determined by the uptake of fluorescent bovine serum albumin (BSA).  $N=6$  biological replicates (with technical duplicates). (A, B) Paired t-test. (C) Click signal as determined by flow cytometry on Rottlerin-treated moDCs incubated for 3 h with 25  $\mu$ M WT HBcAg<sub>18-27</sub>, click HBcAg<sub>18-27</sub> P6 or P9, click SIINFEKL (“clrr”) or DMSO (negative vehicle control).  $N=6$  biological replicates (with technical duplicates). Error bars correspond to the SEM of the biological replicates. Friedman test, Dunnett’s multiple comparisons test. (D) Click signal of each condition with and without the pre-treatment with Rottlerin (10  $\mu$ M).  $N=6$  (with technical duplicates). Paired t test for each condition. \* =  $P \leq 0.05$ , \*\* =  $P \leq 0.01$ , \*\*\* =  $P \leq 0.001$ . MFI = Mean fluorescence intensity.

ratio (Fig. 3D). Taken together, BOC can be used as a tool to visualize and quantify peptides in the context of the HLA complexes on cells.

### BOC can be applied to study processing of synthetic long peptides

Based on the previous experiments, we next determined whether click HBcAg<sub>18-27</sub> analogues P6 and P9 could be used to study APP in moDCs, as this has to date not been possible using click epitopes. In a proof-of-concept experiment, we synthesized 37-amino acid long synthetic long peptides (SLPs) containing the WT, click P6 or P9 HBcAg<sub>18-27</sub> epitope, which require intracellular processing in (mo)DCs to release the HBcAg<sub>18-27</sub> epitopes for loading on HLA to activate T cells.<sup>40,55</sup> This process is made more efficient by the presence of PAMPs, so therefore the immature moDCs were incubated for 1 h or 3 h with TLR1/2 ligand UPam (also known as Amplivant<sup>®</sup><sup>42,43</sup>) and HBcAg<sub>1-37</sub> SLP (containing either the WT, click P6 or P9 HBcAg<sub>18-27</sub> epitope). The minimal epitopes (WT, click P6, or P9 HBcAg<sub>18-27</sub>) were taken along as controls. The cells were washed thoroughly after this pulse period to remove non-cell bound peptides, then fixed, permeabilized, and clicked, either immediately or after a 20 h chase after washing (Fig. 4A; N = 3). Click signal was determined with both flow cytometry and confocal microscopy. Of note, the more limited solubility of SLPs and the need for DMSO, which is cytotoxic at higher concentrations, restricted the (long) peptide concentration in these experiments to 10  $\mu$ M (contrasting the 25  $\mu$ M used for experiments in Fig. 3).

Maturation markers HLA-I, HLA-DR and CD40 were measured by flow cytometry. Like LPS (Pos. ctrl.), UPam potently matured the moDC (Fig. 4B). By flow cytometry, click HBcAg<sub>18-27</sub> SLPs P6 and P9 were observed to be taken up by moDCs within a time-frame as short as 1 h, and signal seemed to decrease already after 3 h of pulse (Fig. 4C). As expected, WT HBcAg<sub>18-27</sub> did not yield any click signal. Contrary to the previous experiments, where cell surface exchanged HLA-A2-associated peptide had been studied on mature moDC (Fig. 3), none of the three short HBcAg<sub>18-27</sub> click analogues yielded click signal upon uptake by these less mature moDC followed by fixation and permeabilization. This discrepancy likely stemmed from the differences in experimental approach (eg, differences in moDC HLA-A2 expression and/or maturation state; peptide concentration (25  $\mu$ M vs 10  $\mu$ M); and permeabilization). After the 20 h chase, click signal was absent in all conditions (Fig. 4D), suggesting dissipation of the signal in absence of newly supplied peptide.

Yet, in order to determine whether the observed signal originated from the cell surface, or rather from an intracellular pool of peptide, confocal microscopy was performed on moDCs after a 3-h pulse and 20-hour chase in this same experiment (N = 3). For this, moDCs were fixed, permeabilized, subjected to CuAAC and co-stained for HLA-I, LAMP1 to mark endo-lysosomal vesicles, and DAPI to visualize nuclei. In line with the flow cytometry results, no click signal was observed for the WT HBcAg<sub>1-37</sub> SLP, nor for any of the 3 short HBcAg<sub>18-27</sub> peptides (Fig. 5A, Fig. S3A-E). For both click HBcAg<sub>1-37</sub> SLPs P6 and P9, however, click signal was substantial, indicating microscopy exceeded in sensitivity over flow cytometry. To assess the location of the click signal, we performed colocalization analyses on the SLP

conditions using the JaCoP plugin in ImageJ.<sup>44</sup> We performed these analyses on both the cross section and on the full Z-stacks, as JaCoP handles the Z-stacks as a volume and returns one colocalization value for the whole 3D (volume) representation (Fig. S4A, B). There were no clear differences between these analyses and therefore we preferred the 3D analyses to give a more representative colocalization value for the whole cell. A relatively large part of this signal (0.654  $\pm$  0.102 and 0.624  $\pm$  0.124 for click SLPs P6 and P9, respectively; Manders' M<sub>1</sub> coefficients, mean  $\pm$  SEM for the 3 biological replicates) seemed to co-localize with HLA-I on the moDC cell surface (Fig. 5B, Table S1), possibly reflecting the HBcAg<sub>18-27</sub> epitope within the HLA-I binding groove after processing and loading on HLA of the SLPs. Interestingly, only a small fraction of the total HLA-I signal (0.104  $\pm$  0.031 and 0.134  $\pm$  0.027 for click SLPs P6 and P9, respectively; Manders' M<sub>2</sub> coefficients, mean  $\pm$  SEM for the three biological replicates) co-localized with the click signal, suggesting that, if the click signal indeed stems from processed and presented HBcAg<sub>18-27</sub> epitope, surface appearance of pHLA complexes on the moDCs is not uniform. While there was colocalization of click signal with HLA-I expression, no colocalization was observed with LAMP1 (Fig. 5B, Table S1), indicating that the SLPs were not specifically present in endo-lysosomes, but rather localized on the cell membrane and in the cytosol. Taken together, we demonstrate that it is feasible to use BOC to study APP with sufficient sensitivity for both flow cytometric and microscopic read-outs.

### Discussion

In conclusion, the herein described click HBcAg<sub>18-27</sub> peptides are promising tools to study APP. Every amino acid in the epitope could be replaced with an alkyne handle with minor effects on HLA-A2 binding affinity, and most positions could be modified without loss of HBcAg<sub>18-27</sub> cognate TCR recognition. Using a novel, robust on-cell click reaction assay, we showed that modification of positions 6 and 9 allowed for a click reaction with the peptide in the HLA-A2 complex on the surface of primary human moDCs. Furthermore, we applied our new tool to track the uptake, processing, and presentation of Hpg-modified SLPs within these moDCs. To our knowledge, these click reactive epitopes compose the first feasible model system that provides a promising outlook to fully track immunogenic, HLA-A2 restricted epitopes through the whole antigen processing and presentation pathways.

The positional scanning of HBcAg<sub>18-27</sub> analogues showed that each amino acid can be replaced with an Hpg click handle without loss of HLA-A2 binding. However, several modifications resulted in slightly reduced affinity for HLA-A2, either due to reduced maximal surface HLA stabilization (positions 1, 2, 4, 5, and 8) or to higher EC<sub>50</sub> values (positions 8 and 10). Interestingly, the anchor residues could be replaced with Hpg, despite their importance for peptide binding. We hypothesize that Hpg, which has a hydrophobic side chain, can be tolerated by the hydrophobic binding pockets present in HLA-A2. Conservative substitution (ie, substitution by an amino acid with similar biochemical properties) of the anchor residue at position 2 has indeed been shown to be allowed with little effect on the binding affinity.<sup>56</sup> Even though conservative substitutions of the C-terminus anchor residue, as analyzed by Bertoletti et al. (1994), significantly impacted HLA-A2 binding,<sup>57</sup> we here show that the non-canonical

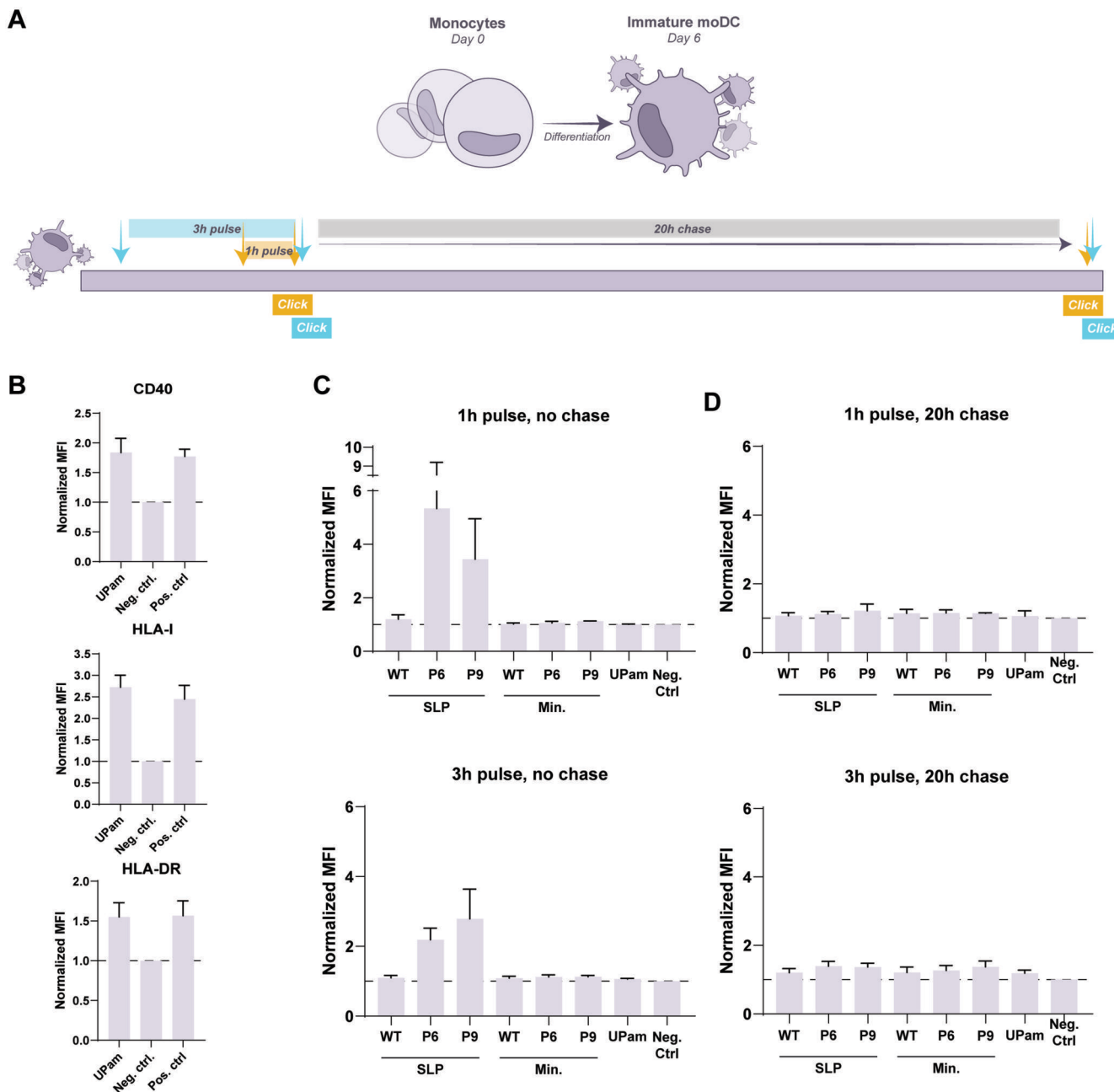


**Figure 4.** Bioorthogonal chemistry can be used to study uptake and processing of synthetic long peptides by flow cytometry. (A) A schematic overview of the pulse-chase experiment performed. moDCs were generated and matured and loaded for either 1 h or 3 h with TLR1/2 ligand Upam (10  $\mu$ M) and HBcAg<sub>18-27</sub> SLPs (10  $\mu$ M) or minimal epitopes (10  $\mu$ M). Click chemistry was performed immediately after pulse, or after 20 h of chase. (B) Maturation of the moDCs was assessed by expression of CD40, HLA-I and HLA-DR. The MFI values were normalized to the negative control (vehicle). (C) Click signals as immediately measured by flow cytometry after moDCs were pulsed for either 1 h (upper panel) or 3 h (lower panel) with HBcAg<sub>18-27</sub> SLPs or minimal epitopes. MFI values were normalized to the negative control (vehicle). (D) Same as (C), but after 20 h chase. Bars correspond to the mean  $\pm$  SEM of the biological replicates.  $N=3$  biological replicates (with technical duplicates). MFI = Mean fluorescence intensity.

amino acid Hpg is, in fact, tolerated at this position. Of note, the HBcAg<sub>18-27</sub> epitope used in this study is a strong HLA-A2 binder. For future expansion of this technique to lower affinity epitopes, one could consider the T2 assay at reduced temperatures of 26 °C, which has been shown to increase the sensitivity of the assay.<sup>58-60</sup>

Additionally, the recognition of the HBcAg<sub>18-27</sub> analogues by the HBcAg<sub>18-27</sub> cognate TCR was assessed. An HLA-peptide recognition motif is specific for each TCR clonotype and hence the results presented here are only valid for the specific TCR we used.<sup>61</sup> For this TCR, modification of

positions 4, 5, and 7 with Hpg abrogated HBcAg<sub>18-27</sub>-specific T cell activation. Correspondingly, position 5 has been shown to be most important for pHLA-A2-TCR interactions, followed by positions 4 and 6,<sup>56</sup> demonstrating the biological relevance of bioorthogonal click chemistry. Interestingly, in our study position 6 could be replaced with Hpg without loss of cognate TCR activation. Some, but not all, HBcAg<sub>18-27</sub>-specific TCRs, allowed mutation of position 6,<sup>56</sup> making it likely that also the specific TCR we used relies less on position 6 for recognition and indicating the use of this position might be extended in part to other HBcAg<sub>18-27</sub>-specific

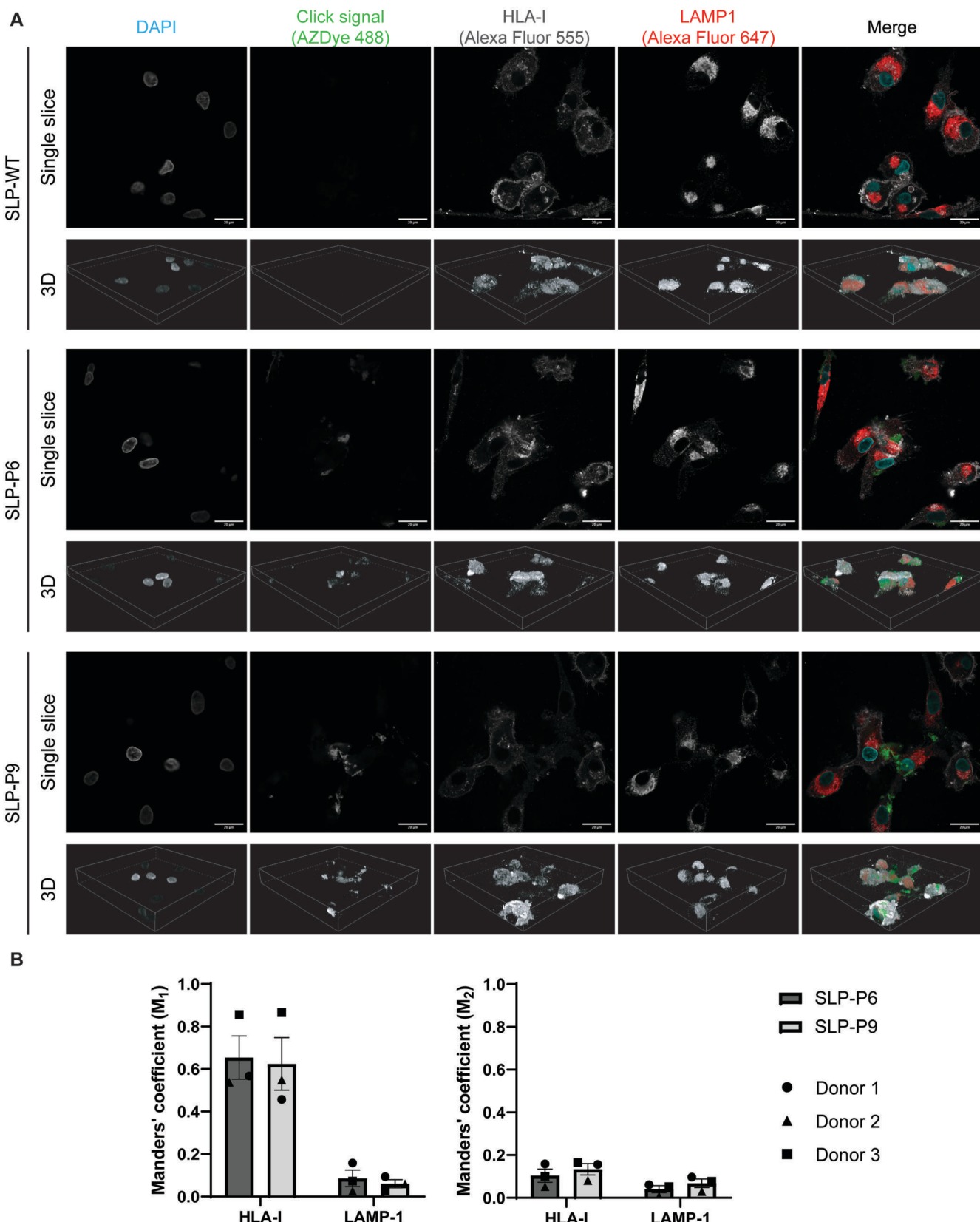


**Figure 5.** Bioorthogonal chemistry can be utilized for epitope tracking by confocal microscopy. moDCs were generated ( $N=3$ ) and matured and loaded for 3 h with  $10\text{ }\mu\text{M}$  TLR1/2 ligand UPam and  $10\text{ }\mu\text{M}$  HBcAg<sub>18-27</sub> SLPs or minimal epitopes ("Min.") and subsequently chased for 20 h. (A) After incubation, cells were fixed with 2% PFA and clicked with  $10\text{ }\mu\text{M}$  AZDye 488 azide (green in merged images) and stained for HLA-I (gray in merged images) and LAMP1 (red in merged images). Nuclei were counterstained with DAPI (cyan in merged images). Full-cell Z-stacks were recorded at  $100\times$  magnification. Z-stacks consisted of on average 76 slices. The images shown are representative images from Donor 2. Three (SLP-WT) or 5 fields (SLP-P6 and SLP-P9) of view (FOV) were imaged per condition, with 4 to 16 cells per FOV. Scale bar:  $20\text{ }\mu\text{m}$ . Images presented are a single slice taken from the Z-stacks and a 3D representation created by volume rendering. (B) Manders' colocalization coefficients were determined to evaluate signal overlap. Manders' coefficient  $M_1$  is the fraction of the click signal overlapping with the marker, and Manders' coefficient  $M_2$  is the fraction of the marker overlapping with the click signal. Values were calculated with the JaCoP plugin in imageJ, using the full Z-stacks as input.  $N=3$  biological replicates, with 2 (Donor 1) or 5 (Donors 2 and 3) FOVs analyzed per condition. Bars correspond to the mean  $\pm$  SEM of the biological replicates.

TCRs.<sup>39</sup> Position 7 has been linked to HBV immune escape in HLA-A2 positive chronic HBV patients,<sup>62</sup> suggesting that this position may still be important for TCR activation.

A previous attempt to develop a click reactive epitope for murine MHC-I did not result in a single click peptide that could both be recognized by the cognate TCR as well as be visualized in the pMHC complex.<sup>23</sup> It is important to note that the alkyne handle used in this study was different than the one used in the present study (propargylglycine (Pg) and Hpg, respectively). Compared to Pg, Hpg has a slightly elongated side chain. The longer side chain of Hpg can possibly adopt more conformations in the pHMA-I complex due to an extra rotatable bond. This would allow the click peptide to adopt more conformations where the relatively bulky alkyne is not interfering with HLA and/or TCR binding, providing a rationale for the use of Hpg over Pg as alkyne handle to design future click epitopes.

Earlier studies have shown that signal-to-noise ratios are problematic for click pMHC complexes,<sup>20,23</sup> even with the best performing click-fluorophore (ie, CalFluor 488, which increases in fluorescence 173× upon being clicked).<sup>52</sup> We have tried multiple approaches to improve the signal-to-noise ratios, among which using the T2 cells as APC and a live-cell compatible copper click reaction.<sup>63</sup> Most of these approaches, however, resulted in poor to no signal. To optimize the BOC pipeline, we opted to use moDCs, which are known to express large amounts of HLA-I on the surface. Furthermore, we decreased background signal using an FPE inhibitor to make sure we only probed pHMA complexes on the surface but not internalized peptide. Finally, we would like to note that also thorough washing to prevent peptide sticking to the outside of the cell and the speed of sample preparation (ie, fixation, blocking, click reaction) and measurement are likely important, as the peptide might fall out of the pHMA complex over time, despite chemical fixation, especially after the ligation of the bulky fluorophore through the click reaction. Our pipeline generated robust and reproducible data, demonstrating that click-modified epitopes HBcAg<sub>18-27</sub> P6 and P9 are available for bioorthogonal ligation in HLA-A2.

Based on the crystal structure, position 6 was not identified as solvent accessible, yet it was clickable in HLA-A2. The alkyne handle might have a different conformation compared to the WT phenylalanine due to a change in biochemical and -physical properties of the sidechain, resulting in unpredicted solvent accessibility of the click handle. Of note, the other solvent-exposed, modified positions that were not taken along in our on-cell click assay because of loss of TCR-recognition and/or reduced HLA-binding (ie, positions 1, 4, 5 and 8) might still be available for CuAAC ligation in the pHMA complex.

For future studies the library of click epitopes should be expanded, especially to other HLA supertypes, in order to get a more comprehensive view of APP. The herein presented workflow should provide a strong basis for the development of click epitopes restricted to other HLA types. The limiting step, however, could be an HLA binding assay, as the T2 assay is only available for a selection of HLA types.<sup>64,65</sup> An alternative approach could be to use UV-cleavable HLA binding assays that make use of stabilized HLA complexes and an MS-based approach.<sup>66,67</sup> Furthermore, cognate T cell recognition as well as on-cell click provide evidence that a peptide is HLA-bound, omitting the need for an HLA binding assay all together.

As a proof of concept of our BOC pipeline, we incorporated the identified click epitopes in a model SLP to study the

uptake and degradation of SLPs. Several SLP-based therapeutic vaccines are currently being clinically tested and for next generation vaccine design it is important to better understand how to achieve optimal SLP processing and presentation.<sup>22,68</sup> We used flow cytometry to show that SLPs are taken up rapidly (ie, within 1 h) by moDCs and that signal decreases quickly (already after 3 h) and after 20 h is not detected anymore by flow cytometry. This suggests that the SLP and the click handle are either degraded very quickly, or regurgitated back into the medium, as DCs are known to do.<sup>69,70</sup>

Interestingly, using confocal microscopy, signal from the click handles could still be detected after a 20 h chase and was co-localizing for a large part with HLA-I. Unfortunately, the resolution of confocal imaging is not sufficient to show precise co-localization. For this, a method that can overcome the diffraction limit would be needed. Here, 2-color single molecule localization microscopy to determine colocalization of the click and HLA-I signals in the nm range on the surface of moDCs may be the answer.<sup>71</sup> It should be noted, however, that these experiments were aimed at following intracellular processing rather than presentation and hence were performed on moDCs with unknown and variable HLA types. Therefore, besides HLA-A2 also other HLA-I alleles might be available to present other SLP-derived epitopes containing the click handle (eg, HLA-B07).<sup>72</sup> However, the used pan-HLA-I staining should account for such other HLA-I types as well and thus our colocalizations should hold. Furthermore, in contrast to the on-cell click experiment, uptake was now not inhibited and consequently also HLA-II (eg, HLA-DR1/3/7) might present epitopes containing the click handles.<sup>73</sup>

An alternative approach to microscopy would be the identification of HLA-bound peptides through mass spectrometry (ie, immunopeptidomics).<sup>74</sup> With the recent development of high sensitive methods, HLA-loaded click epitopes can be identified from a relatively small amount of moDCs upon SLP processing and loading. As we demonstrate, the click handle can be detected by mass spectrometry due to its unique mass and structure (Fig. S5 shows the detection of the click handles after synthesis of the SLPs), making this an experimentally straight-forward approach that would allow for the simultaneous tracking of WT and various click variants using the same click handle at different positions. For post hoc analysis, however, search databases do need to include the non-canonical amino acid, which drastically increases the search space.

Notably, after the processing of the SLPs, we observed little to no overlap of click signal with LAMP1 positive vesicles (ie endo-lysosomes) and only some localization in the cytosol. It has recently been shown that SLPs do not need to pass through the lysosome during cross-presentation,<sup>75</sup> supporting our observed lack of localization of the epitope in LAMP1 positive vesicles. Interestingly, Rosalia et al. (2013) used SLPs conjugated to a BODIPY-FL fluorophore and assessed uptake for 3 h or 24 h by murine DCs.<sup>76</sup> The signal of the BODIPY-FL-SLP was located primarily in the cytosol outside endolysosomes and stemmed from unprocessed SLP. We did not observe a similar distribution, possibly due to the inclusion of a chase period for processing, which was not included by Rosalia et al., or, more likely, due to influence of the BODIPY-FL on antigen processing or distribution. Hence this discrepancy enforces the need for a labeling strategy that is less invasive. Moreover, compared to this murine model, our model allows for visualization of both the intact SLP and the

shorter minimal epitope, rather than only the intact SLP. Of note, for discrimination of the two a second click reactive amino acid based on a different click handle could be included outside the minimal HLA-binding epitope. Thus, our model enables tracking of antigen processing from start to finish and is better suited for in-depth studies of antigen processing, routing, and presentation.

Taken together, we believe that the herein described click chemistry-based workflow and HBcAg<sub>18-27</sub> epitopes are novel tools that can be utilized to answer open questions in the field of antigen presentation. For example, it has previously been demonstrated that the conjugation of an TLR2/1 ligand (Amplivant) to SLPs inhibits cross presentation of the HBcAg<sub>18-27</sub> epitope, suggesting alternative processing pathways compared to freely administered SLPs.<sup>55</sup> Incorporating the click epitope in TLR ligand-SLP conjugates could help elucidate the mechanism responsible for this observation, which would be highly insightful to better design SLP-based vaccines. Moreover, our approach allows for the direct comparison of antigen presentation pathways between different APCs. Lastly, the repertoire of click epitopes should be expanded to other HLA-I supertypes and HLA-II restricted epitopes, allowing the study of the whole antigen processing and presentation pathways in a more unbiased manner. The pipeline described in this study should provide a clear guideline for the development of new click reactive epitopes.

## Author contributions

Thijmen P. Mostert (Formal analysis [Equal], Investigation [Equal], Methodology [Equal], Visualization [Equal], Writing—original draft [Equal], Writing—review & editing [Equal]), Amy L. Kessler (Formal analysis [Equal], Investigation [Equal], Methodology [Equal], Visualization [Equal], Writing—original draft [Equal], Writing—review & editing [Equal]), Robbie J. Luijten (Investigation [Equal]), Ward Doelman (Investigation [Equal], Methodology [Equal], Resources [Equal]), Marjolein M. E. Isendoorn (Resources [Equal]), Dmitri V. Filippov (Resources [Equal]), Sander I. van Kasteren (Conceptualization [Equal], Funding acquisition [Equal], Supervision [Equal], Writing—review & editing [Equal]), and Sonja I. Buschow (Conceptualization [Equal], Funding acquisition [Equal], Supervision [Equal], Writing—review & editing [Equal])

## Supplementary material

Supplementary material is available at *The Journal of Immunology* online.

## Funding

S.I.v.K. was funded by European Research Council Grant number 865175.

## Conflicts of interest

S.I.B. is listed as an inventor on a patent application (PCT/EP2020/070957) concerning the application of synthetic long peptides for the treatment of hepatitis B infection filled by ISA pharmaceuticals. S.I.B. collaborates with and/or has received funding from ISA pharmaceuticals b.v., ISAbella

Pharma b.v., Pfizer Inc, Merus n.v., Numab therapeutics AG, Imuno b.v. and VitroScan b.v.

## Data availability

The data that support the findings of this study are available from the corresponding author upon reasonable request.

## References

1. Neeffes J, Jongsma ML, Paul P, Bakke O. Towards a systems understanding of MHC class I and MHC class II antigen presentation. *Nat Rev Immunol.* 2011;11:823–836.
2. Pishesha N, Harmand TJ, Ploegh HL. A guide to antigen processing and presentation. *Nat Rev Immunol.* 2022;22:751–764.
3. Rock KL, Reits E, Neeffes J. Present yourself! By MHC Class I and MHC Class II molecules. *Trends Immunol.* 2016;37:724–737.
4. Hwang J-R, Byeon Y, Kim D, Park S-G. Recent insights of T cell receptor-mediated signaling pathways for T cell activation and development. *Exp Mol Med.* 2020;52:750–761.
5. Pollard AJ, Bijkem EM. A guide to vaccinology: from basic principles to new developments. *Nat Rev Immunol.* 2021;21:83–100.
6. Fan T et al. Therapeutic cancer vaccines: advancements, challenges, and prospects. *Signal Transduct Target Ther.* 2023;8:450.
7. Tian Y, Hu D, Li Y, Yang L. Development of therapeutic vaccines for the treatment of diseases. *Mol Biomed.* 2022;3:40.
8. Kenison JE, Stevens NA, Quintana FJ. Therapeutic induction of antigen-specific immune tolerance. *Nat Rev Immunol.* 2024; 24:338–357.
9. Cruz FM, Chan A, Rock KL. Pathways of MHC I cross-presentation of exogenous antigens. *Semin Immunol.* 2023; 66:101729.
10. Embgenbroich M, Burgdorf S. Current concepts of antigen cross-presentation. *Front Immunol.* 2018;9:1643.
11. Nair-Gupta P et al. TLR signals induce phagosomal MHC-I delivery from the endosomal recycling compartment to allow cross-presentation. *Cell.* 2014;158:506–521.
12. Blander JM, Medzhitov R. Toll-dependent selection of microbial antigens for presentation by dendritic cells. *Nature.* 2006; 440:808–812.
13. Boross P et al. FcRy-Chain ITAM signaling is critically required for cross-presentation of soluble antibody-antigen complexes by dendritic cells. *J Immunol.* 2014;193:5506–5514.
14. Dahan R, Reiter Y. T-cell-receptor-like antibodies—generation, function and applications. *Expert Rev Mol Med.* 2012;14:e6.
15. Li Y, Jiang W, Mellins ED. TCR-like antibodies targeting autoantigen-mhc complexes: a mini-review. *Front Immunol.* 2022; 13:968432.
16. Norbury CC, Chambers BJ, Prescott AR, Ljunggren H-G, Watts C. Constitutive macropinocytosis allows TAP-dependent major histocompatibility complex class I presentation of exogenous soluble antigen by bone marrow-derived dendritic cells. *Eur J Immunol.* 1997;27:280–288.
17. Giordini A, Cresswell P. Hsp90-mediated cytosolic refolding of exogenous proteins internalized by dendritic cells. *Embo J.* 2008; 27:201–211.
18. Sanchez-Rico C, Voith von Voithenberg L, Warner L, Lamb DC, Sattler M. Effects of fluorophore attachment on protein conformation and dynamics studied by spFRET and NMR spectroscopy. *Chemistry.* 2017;23:14267–14277.
19. van Leeuwen T et al. Bioorthogonal protein labelling enables the study of antigen processing of citrullinated and carbamylated auto-antigens. *RSC Chem Biol.* 2021;2:855–862.
20. Baranov MV et al. The phosphoinositide kinase PIKfyve promotes Cathepsin-S-mediated major histocompatibility complex class II antigen presentation. *iScience.* 2019;11:160–177.
21. Castelvecchi D, Ledford H. Chemists who invented revolutionary “click” reactions win Nobel. *Nature.* 2022;610:242–243.

22. Hos BJ, Tondini E, van Kasteren SI, Ossendorp F. Approaches to improve chemically defined synthetic peptide vaccines. *Front Immunol.* 2018;9:884.
23. Pawlak JB et al. The optimization of bioorthogonal epitope ligation within MHC-I complexes. *ACS Chem Biol.* 2016; 11:3172–3178.
24. Sletten EM, Bertozzi CR. Bioorthogonal chemistry: fishing for selectivity in a sea of functionality. *Angew Chem Int Ed.* 2009; 48:6974–6998.
25. Scinto SL, et al. Bioorthogonal chemistry. *Nat Rev Methods Primers.* 2021;1:30.
26. Bird RE, Lemmel SA, Yu X, Zhou QA. Bioorthogonal chemistry and its applications. *Bioconjug Chem.* 2021;32:2457–2479.
27. Boyce M, Bertozzi CR. Bringing chemistry to life. *Nat Methods.* 2011;8:638–642.
28. Meldal M, Tornøe CW. Cu-catalyzed azide-alkyne cycloaddition. *Chem Rev.* 2008;108:2793–3442.
29. Rostovtsev VV, Green LG, Fokin VV, Sharpless KB. A stepwise huisgen cycloaddition process: Copper(I)-catalyzed regioselective “ligation” of azides and terminal alkynes. *Angew Chem Int Ed.* 2002;41:2596–2599.
30. Bakum T et al. Quantification of bioorthogonal stability in immune phagocytes using flow cytometry reveals rapid degradation of strained alkynes. *ACS Chem Biol.* 2018; 13:1173–1179.
31. van Hest JCM, Kiick KL, Tirrell DA. Efficient incorporation of unsaturated methionine analogues into proteins in vivo. *J Am Chem Soc.* 2000;122:1282–1288.
32. Bertheussen K et al. Live-cell imaging of sterculic acid—a naturally occurring 1,2-cyclopropene fatty acid—by bioorthogonal reaction with turn-on tetrazine-fluorophore conjugates. *Angew Chem Int Ed.* 2022;61:e202207640.
33. Croce S, Serdjukow S, Carell T, Frischmuth T. Chemoenzymatic preparation of functional click-labeled messenger RNA. *Chembiochem.* 2020;21:1641–1646.
34. Tsuchiya M, Tachibana N, Hamachi I. Post-click labeling enables highly accurate single cell analyses of glucose uptake ex vivo and in vivo. *Commun Biol.* 2024;7:459.
35. He Z et al. Metabolic labeling and imaging of cellular RNA via bioorthogonal cyclopropene-tetrazine ligation. *CCS Chem.* 2020; 2:89–97.
36. Seul N et al. Cyclopropenes as chemical reporters for dual bioorthogonal and orthogonal metabolic labeling of DNA. *Angew Chem Int Ed.* 2024;63:e202403044.
37. Salter RD, Howell DN, Cresswell P. Genes regulating HLA class I antigen expression in T-B lymphoblast hybrids. *Immunogenetics.* 1985;21:235–246.
38. Bernabeu C, van de Rijn M, Lerch PG, Terhorst CP.  $\beta_2$ -Microglobulin from serum associates with MHC class I antigens on the surface of cultured cells. *Nature.* 1984;308:642–645.
39. Banu N et al. Building and optimizing a virus-specific T cell receptor library for targeted immunotherapy in viral infections. *Sci Rep.* 2014;4:4166.
40. Dou Y et al. HBV-derived synthetic long peptide can boost CD4<sup>+</sup> and CD8<sup>+</sup> T-cell responses in chronic HBV patients ex vivo. *J Infect Dis.* 2018;217:827–839.
41. Gehring AJ et al. Engineering virus-specific T cells that target HBV infected hepatocytes and hepatocellular carcinoma cell lines. *J Hepatol.* 2011;55:103–110.
42. Willems MM et al. N-tetradecylcarbamyl lipopeptides as novel agonists for Toll-like receptor 2. *J Med Chem.* 2014;57: 6873–6878.
43. Zom GG et al. TLR2 ligand-synthetic long peptide conjugates effectively stimulate tumor-draining lymph node T cells of cervical cancer patients. *Oncotarget.* 2016;7:67087–67100.
44. Bolte S, Cordelieres FP. A guided tour into subcellular colocalization analysis in light microscopy. *J Microsc.* 2006; 224:213–232.
45. Madden DR, Garboczi DN, Wiley DC. The antigenic identity of peptide-MHC complexes: a comparison of the conformations of five viral peptides presented by HLA-A2. *Cell.* 1993; 75:693–708.
46. Pettersen EF et al. UCSF Chimera—a visualization system for exploratory research and analysis. *J Comput Chem.* 2004;25: 1605–1612.
47. Cerundolo V et al. Presentation of viral antigen controlled by a gene in the major histocompatibility complex. *Nature.* 1990; 345:449–452.
48. Hosken NA, Bevan MJ. Defective presentation of endogenous antigen by a cell line expressing class I molecules. *Science.* 1990; 248:367–370.
49. Eisen HN et al. Promiscuous binding of extracellular peptides to cell surface class I MHC protein. *Proc Natl Acad Sci U S A.* 2012; 109:4580–4585.
50. Santambrogio L, Sato AK, Fisher FR, Dorf ME, Stern LJ. Abundant empty class II MHC molecules on the surface of immature dendritic cells. *Proc Natl Acad Sci U S A.* 1999;96: 15050–15055.
51. D. P M, Esquivel F, Lukszo J, Bennink JR, Yewdell JY. Effect of TAP on the generation and intracellular trafficking of peptide-receptive major histocompatibility complex class I molecules. *Immunity.* 1995;5:137–147.
52. Shieh P et al. CalFluors: a universal motif for fluorogenic azide probes across the visible spectrum. *J Am Chem Soc.* 2015; 137:7145–7151.
53. Diken M et al. Selective uptake of naked vaccine RNA by dendritic cells is driven by macropinocytosis and abrogated upon DC maturation. *Gene Ther.* 2011;18:702–708.
54. Sarkar K, Kruhlak MJ, Erlandsen SL, Shaw S. Selective inhibition by rottlerin of macropinocytosis in monocyte-derived dendritic cells. *Immunology.* 2005;116:513–524.
55. Dou Y et al. Design of TLR2-ligand-synthetic long peptide conjugates for therapeutic vaccination of chronic HBV patients. *Antiviral Res.* 2020;178:104746.
56. Bertoletti A et al. Molecular features of the hepatitis B virus nucleocapsid T-cell epitope 18-27: interaction with HLA and T-cell receptor. *Hepatology.* 1997;26:1027–1034.
57. Bertoletti A et al. Cytotoxic T lymphocyte response to a wild type hepatitis B virus epitope in patients chronically infected by variant viruses carrying substitutions within the epitope. *J Exp Med.* 1994;180:933–943.
58. Ljunggren H-G et al. Empty MHC class I molecules come out in the cold. *Nature.* 1990;346:476–480.
59. Stuber G et al. Identification of wild-type and mutant p53 peptides binding to HLA-A2 assessed by a peptide loading-deficient cell line assay and a novel major histocompatibility complex class I peptide binding assay. *Eur J Immunol.* 1994;24:765–768.
60. Wei ML, Cresswell P. HLA-A2 molecules in an antigen processing mutant cell contain signal sequence-derived peptides. *Nature.* 1992;356:443–446.
61. Gray GI et al. The evolving T cell receptor recognition code: the rules are more like guidelines. *Immunol Rev.* 2025;329:e13439.
62. Kefalakes H et al. Adaptation of the hepatitis B virus core protein to CD8(+) T-cell selection pressure. *Hepatology.* 2015;62:47–56.
63. Besanceney-Webler C et al. Increasing the efficacy of bioorthogonal click reactions for bioconjugation: a comparative study. *Angew Chem Int Ed.* 2011;50:8051–8056.
64. Chen H-W et al. Identification of HLA-A11-restricted CTL epitopes derived from HPV type 18 using DNA immunization. *Cancer Biol Ther.* 2009;8:2025–2032.
65. Kuzushima K, Hayashi N, Kimura H, Tsurumi T. Efficient identification of HLA-A\*2402-restricted cytomegalovirus-specific CD8<sup>+</sup> T-cell epitopes by a computer algorithm and an enzyme-linked immunospot assay. *Blood.* 2001;98:1872–1881.
66. Rodenko B et al. Generation of peptide-MHC class I complexes through UV-mediated ligand exchange. *Nat Protoc.* 2006; 1:1120–1132.
67. Toebes M et al. Design and use of conditional MHC class I ligands. *Nat Med.* 2006;12:246–251.

68. Hamley IW. Peptides for vaccine development. *ACS Appl Bio Mater.* 2022;5:905–944.
69. El-Barbry H et al. Extracellular release of antigen by dendritic cell regurgitation promotes B cell activation through NF- $\kappa$ B/cRel. *J Immunol.* 2020;205:608–618.
70. Le Roux D et al. Antigen stored in dendritic cells after macropinocytosis is released unprocessed from late endosomes to target B cells. *Blood.* 2012;119:95–105.
71. Lelek M et al. Single-molecule localization microscopy. *Nat Rev Methods Primers.* 2021;1:39.
72. Bertoni R et al. Human histocompatibility leukocyte antigen-binding supermotifs predict broadly cross-reactive cytotoxic T lymphocyte responses in patients with acute hepatitis. *J Clin Invest.* 1997;100:503–513.
73. Godkin A, Davenport M, Hill AVS. Molecular analysis of HLA class II associations with hepatitis B virus clearance and vaccine nonresponsiveness. *Hepatology.* 2005; 41:1383–1390.
74. Shapiro IE, Bassani-Sternberg M. The impact of immunopeptidomics: from basic research to clinical implementation. *Semin Immunol.* 2023;66:101727.
75. Lighart NAM et al. A lysosome-targeted tetrazine for organelle-specific click-to-release chemistry in antigen presenting cells. *J Am Chem Soc.* 2023;145:12630–12640.
76. Rosalia RA et al. Dendritic cells process synthetic long peptides better than whole protein, improving antigen presentation and T-cell activation. *Eur J Immunol.* 2013; 43:2554–2565.